Available online at www.sciencedirect.com
ScienceDirect
Carbohydrate Research 343 (2008) 685–694
Carbohydrate RESEARCH

Synthesis and evaluation of Gd-DTPA-labeled arabinogalactans as potential MRI contrast agents

Weisheng Li,[a,b] Zhongfeng Li,[a,b] Fengying Jing,[a] Yuefeng Deng,[a] Lai Wei,[a,b] Peiqiu Liao,[a,b] Xiangguang Yang,[a] Xiaojing Li,[a,*] Fengkui Pei,[a,*] Xuxia Wang[b,c] and Hao Lei[c]

[a]*Changchun Institute of Applied Chemistry, Chinese Academy of Sciences, Changchun 130022, PR China*
[b]*Graduate School of the Chinese Academy of Sciences, Beijing 10039, PR China*
[c]*State Key Laboratory of Magnetic Resonance and Atomic and Molecular Physics, Wuhan Institute of Physics and Mathematics, Chinese Academy of Sciences, Wuhan 430071, PR China*

Received 30 August 2007; received in revised form 1 January 2008; accepted 8 January 2008
Available online 16 January 2008

Abstract—Arabinogalactan derivatives conjugated with gadolinium-diethylenetriaminepentaacetic acid (Gd-DTPA) by ethylenediamine (Gd-DTPA-CMAG-A_2) or hexylamine (Gd-DTPA-CMAG-A_6) have been synthesized and characterized by means of Fourier transform infrared spectra (FTIR), ^{13}C nuclear magnetic resonance (^{13}C NMR), size exclusion chromatography (SEC), and inductively coupled plasma atomic emission spectrometry (ICP-AES). Relaxivity studies showed that arabinogalactan-bound complexes possessed higher relaxation effectiveness compared with the clinically used Gd-DTPA, and the influence of the spacer arm lengths on the T_1 relaxivities was studied. Their stability was investigated by competition study with Ca^{2+}, EDTA, and DTPA. MR imaging of Wistar rats showed remarkable enhancement in rat liver and kidney after i.v. injection of Gd-DTPA-CMAG-A_2 (0.079 ± 0.002 mmol/kg Gd^{3+}): The mean percentage enhancement of the liver parenchyma and kidney was $38.7 \pm 6.4\%$ and $69.4 \pm 4.4\%$ at 10–30 min. Our preliminary in vivo and in vitro study indicates that the arabinogalactan-bound complexes are potential liver-specific contrast agents for MRI.

Keywords: Magnetic resonance imaging; Contrast agent; Liver-specific; Arabinogalactan; Relaxivity

1. Introduction

Magnetic resonance imaging (MRI) is one of the most useful diagnostic techniques in clinical medicine because it allows researchers and doctors to image the body in a noninvasive manner.[1,2] Image quality can be enhanced by the administration of contrast agents, which enhance various portions of the MR image by changing, usually decreasing, the relaxation time of the tissue water and, thus, allowing the area of interest to be much more conspicuous than the surrounding tissues. Currently, more than 35% of all MRI examinations are accompanied by administration of contrast agents.[3] Up to now, four kinds of gadolinium complexes (Gd-DTPA, Gd-DTPA-BMA, Gd-DOTA, and Gd-HPDO3A) have been used worldwide for intravenous administration. These comparatively small molecular agents have been used successfully to enhance the imaging of brain and central nervous system. However, these small hydrophilic complexes are nonspecific extracellular contrast agents and are excreted rapidly through the kidneys, which may limit their use in other parts of the body. Therefore, there is a significant need for agents that target specific organs, regions of the body, or diseased tissue to gain the greatest diagnostic value.[4–7] In recent years, the research and development for liver-specific contrast agents with high relaxivities and kinetic stability have been quite active.[8–11] Some groups became

* Corresponding authors. Tel.: +86 431 8526 2219; fax: +86 431 8568 5653 (F.P.); e-mail addresses: xjli@ciac.jl.cn; peifk@ciac.jl.cn

0008-6215/$ - see front matter © 2008 Elsevier Ltd. All rights reserved.
doi:10.1016/j.carres.2008.01.008

interested in contrast agents which enter hepatocytes through hepatic asialoglycoprotein receptor (ASGP-R), which is an organ-specific lectin, not found anywhere in the body except on the surface of hepatocytes.[12–14] Arabinogalactan, a polysaccharide isolated from plants, is known to be specifically absorbed by hepatocytes via the ASGP-R. The presence of numerous terminal galactose residues and the high degree of branching of arabinogalactan are responsible for its bindings to the ASGP-R.[15] The polysaccharide and its derivatives have been used as carriers to deliver drugs to hepatocytes via this receptor.[16,17] A spin-labelled arabinogalactan,[12] as well as an arabinogalactan-stabilized ultrasmall superparamagnetic iron oxide (AG-USPIO)[13] has been reported as liver-specific contrast agents for MRI by targeting hepatocyte ASGP-R.

We had previously described Gd-DTPA directly linked to natural polysaccharides via ester bonds as contrast agents for MRI.[18,19] As a continuation, the aims of this study were to synthesize arabinogalactan-linked Gd-DTPA (Gd-DTPA-CMAG-A_n; $n = 2$ or $n = 6$) connected via amide groups. The influence of the spacer arm lengths and Ca^{2+}, EDTA, or DTPA on the r_1 relaxivity were investigated. Furthermore, we evaluated the potential application of Gd-DTPA-CMAG-A_2 as a liver-specific contrast agent by in vivo experiments.

2. Results and discussion

2.1. Characterization of DTPA-CMAG-A_n

There are several structural types of arabinogalactans.[20,21] Generally, type I and type II of AG are distinguished. The ^{13}C NMR spectrum (Fig. 1) of the AG used in this work is similar as those reported from Larch species (type II).[22,23] The AG has a framework of β-(1→3) D-galactopyranose residues branched at C-6. The side chains consist of single β-D-Gal*p* or dimer structures such as β-Gal*p*-(1→6)-β-Gal*p*, β-Ara*p*-(1→3)-Ara*f*, and β-Ara*p*-(1→3)-Ara*f*.[20]

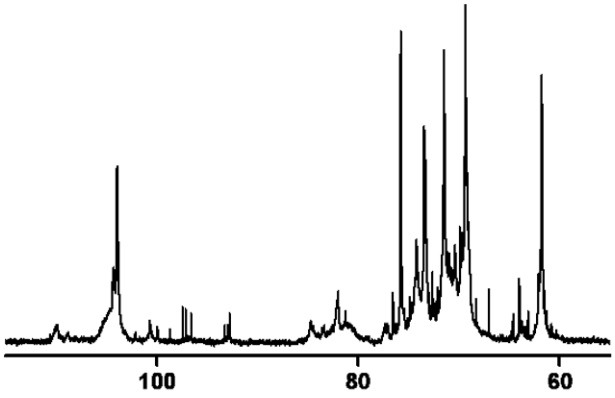

Figure 1. ^{13}C NMR spectrum of AG in 4:1 water–D_2O.

The synthetic route to arabinogalactan-linked Gd-DTPA as MRI contrast agents is depicted in Scheme 1. The DTPA-CMAG-A_2 was characterized by size exclusion chromatography as shown in Figure 2. DTPA-CMAG-A_2 eluted as a single peak with a retention time of 16.5 min, compared to Dextran T-10 (molecular weight: 10 kD) and Dextran T-40 (molecular weight: 40 kD) standards (16.7 and 15.4 min, respectively). The starting arabinogalactan eluted at 16.1 min (spectrum not shown) and a small amount of a low molecular weight arabinogalactan was removed by dialysis. DTPA-CMAG-A_6 eluted at 16.4 min (spectrum not shown) and exhibited an elution profile similar to DTPA-CMAG-A_2.

The FTIR spectra of AG and its derivatives (CMAG, CMAG-A_2, and DTPA-CMAG-A_2) are shown in Figure 3. Arrows point out to some characteristic vibrations.[24,25] The successful incorporation of carboxylate groups onto AG block was verified by the appearance of a peak at 1604 cm^{-1} in the spectrum of CMAG (b). The spectrum of CMAG-A_2 (c) presents a peak at 1650 cm^{-1}, attributed to the –NHCO (amide I), which indicates that the acylamino bond in CMAG-A_2 was formed. After CMAG-A_2 linking to DTPA, the peak appeared at 1738 cm^{-1}, corresponding to the carboxylate in DTPA (d).

The structure of the synthesized polymers was further supported by the ^{13}C NMR spectra. Compared to AG alone, two additional peaks of CMAG at 178.6–177.7 and 68.7 ppm were assigned to COONa and CH_2 carbon atoms of a carboxymethyl ester.[26] The ^{13}C NMR spectrum of CMAG-A_2 exhibited three new peaks at 173.7, 40.7, and 39.9 ppm, corresponding to the carbonyl CONH, the amido α-carbon $NHCH_2$, and the amino α-carbon CH_2NH_2,[27] respectively. The spectrum still contained peaks at 178.6–177.7 ppm, consistent with residual unsubstituted COONa. In the case of DTPA-CMAG-A_2, the peak corresponding to the amino α-carbon disappeared, an indication that all of the CMAG-A_2 amino groups were substituted by DTPA. Some new peaks were observed with the following possible assignments (see Scheme 1):[28,29] 179.2 and 171.2 ppm, the C-1 and C-7 (C-7′, C-7″) of DTPA carboxyls; 60.9, 57.7, 56.8, 53.6, and 49.0 ppm, the C-5, C-6 (C-6′, C-6″), C-2, C-3 (C-3′), and C-4 (C-4′) of DTPA CH_2 carbons.

The IR and ^{13}C NMR results indicated that DTPA was linked to aminated arabinogalactan by an amide function.

The contents of AG derivatives were determined by quantitative assays. The synthesized CMAG sample contained 2.0 mmol of COONa/g. Samples CMAG-A_2 (CMAG-A_6) contained 0.51 (0.50) mmol of NH_2/g and so the residual unsubstituted COONa groups were

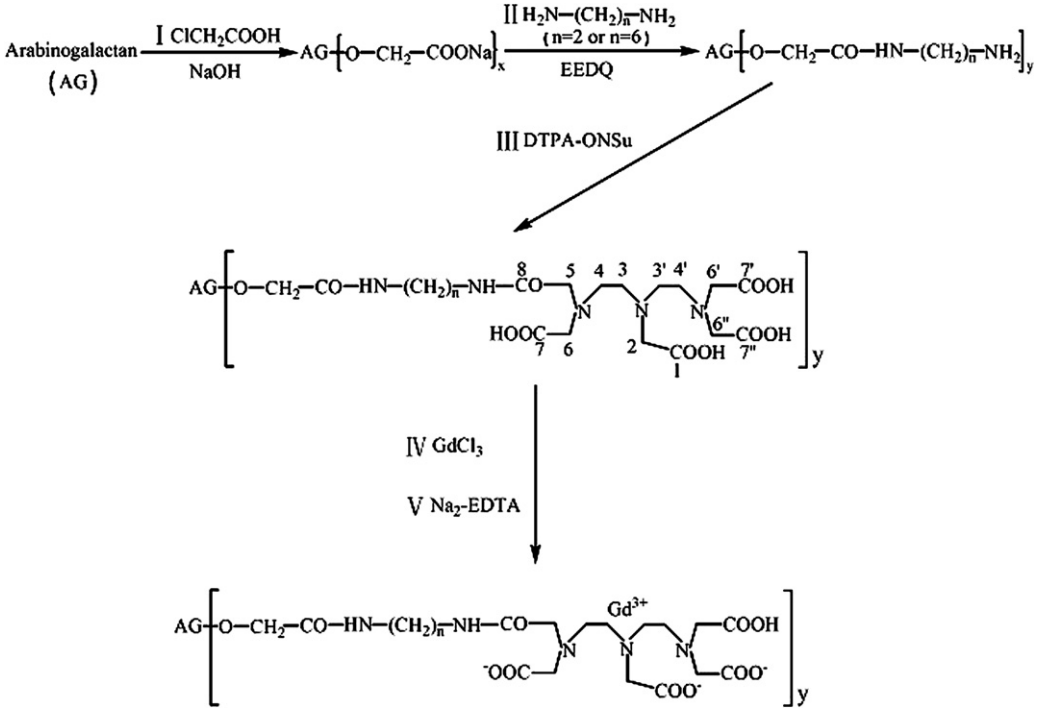

Scheme 1. The synthesis route to arabinogalactan-linked Gd-DTPA.

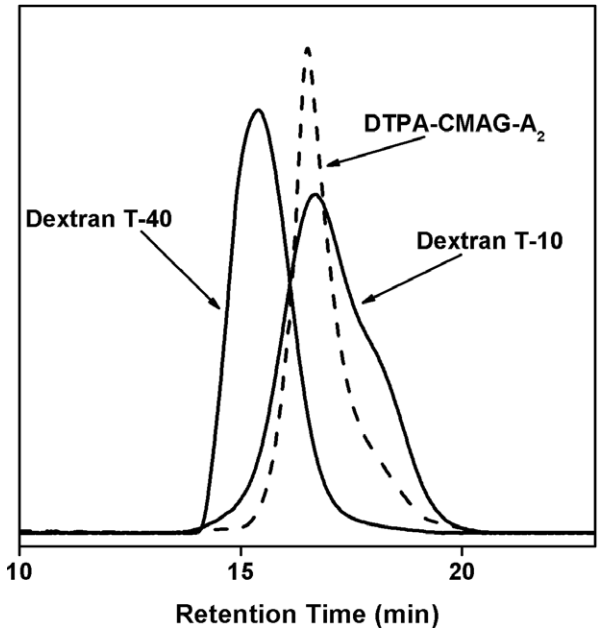

Figure 2. Size exclusion chromatography of DTPA-CMAG-A_2.

about 1.5 mmol/g. The average number of DTPA-bound arabinogalactan was determined by a back-titration procedure using EDTA as well as ICP-AES. The results showed that DTPA-CMAG-A_2 (DTPA-CMAG-A_6) had 0.51 (0.50) mmol of DTPA/g, respectively, indicating good agreement between the two methods.

2.2. Relaxivity

The T_1-relaxivities of Gd-DTPA-CMAG-A_n in D_2O and 0.725 mM bovine serum albumin (BSA) solutions are listed in Table 1. The relaxivity of Gd-DTPA-CMAG-A_n in D_2O is higher than that of commercial contrast agent Gd-DTPA. Possible explanations for increased relaxivities, relative to Gd-DTPA, include (a) an increase in rotational correlation time by virtue of the attachment of the metal chelate to macromolecules, (b) an increase in the number of inner sphere coordinated water molecules, (c) an increase in the number of outer sphere coordinated water molecules via entrapment by the polysaccharide.[2,30,31] However, compared with that of dendrimer-based agents,[32,33] the relaxivities of Gd-DTPA-CMAG-A_n were lower because the linear characteristic of the polysaccharide makes the part of Gd-DTPA easier to rotate, which partly reduces the relaxivity resulting from increase of the rotational correlation time of the chelated part of the metal.

Serum albumin is the richest protein of mammal blood plasma and plays a crucial role in the uptake, transportation, biodistribution, and excretion of the contrast agent in human body.[34] The relaxation time (T_1) for various concentrations of Gd-DTPA-CMAG-A_n (0–1.5 mM) in 0.725 mM BSA solution was measured. The relaxivity can also be obtained from the linear regression according to Eq. 1. Table 1 illustrates a reasonable enhancement of solvent proton relaxation rates for Gd-DTPA-CMAG-A_n in BSA solution. It

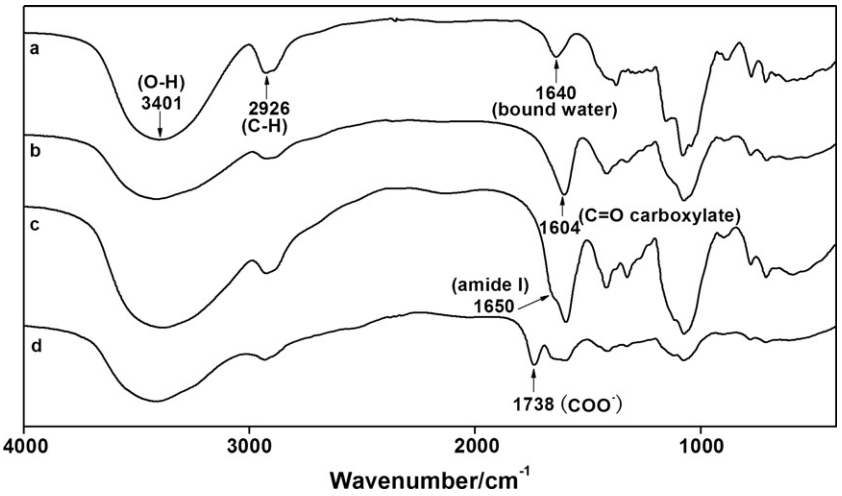

Figure 3. The FTIR spectra of AG (a); CMAG (b); CMAG-A_2 (c); and DTPA-CMAG-A_2 (d).

Table 1. The T_1-relaxivities r_1 ($mM^{-1}\,s^{-1}$) of Gd-DTPA and Gd-DTPA-CMAG-A_n[a]

Gd^{3+} complexes	The T_1-relaxivities r_1 ($mM^{-1}\,s^{-1}$)	
	In D_2O	In 0.725 mM BSA
Gd-DTPA	5.3	5.4
Gd-DTPA-CMAG-A_2	7.4	7.9
Gd-DTPA-CMAG-A_6	7.3	7.6

[a] The proton relaxivities r_1 were measured at 400 MHz and 25 °C.

is 7.9 $mM^{-1}\,s^{-1}$ for Gd-DTPA-CMAG-A_2 and 7.6 $mM^{-1}\,s^{-1}$ for Gd-DTPA-CMAG-A_6 with a correlation coefficient better than 0.99, which is 1.07 and 1.04 times that of Gd-DTPA-CMAG-A_2 and Gd-DTPA-CMAG-A_6 in D_2O. It is very likely that other paramagnetic species exist in BSA solution besides free Gd-DTPA-CMAG-A_n. Since the equilibrium constant for the binding of Gd^{3+} to the serum albumin is very small relative to the stability constant of Gd-DTPA-CMAG-A_n,[35] the possible release of Gd^{3+} from Gd-DTPA-CMAG-A_n could be ignored. Above enhancement is attributable to Gd-DTPA-CMAG-A_n being noncovalently bound to BSA. Using the method of Feng et al.[36] it was deduced that about 4.0% of Gd-DTPA-CMAG-A_2 and about 2.7% of Gd-DTPA-CMAG-A_6 exist as Gd-DTPA-CMAG-A_2·BSA or Gd-DTPA-CMAG-A_6·BSA under the condition of [BSA] = 0.725 mM with equilibrium constants of 0.0579 and 0.0372 mM^{-1}, respectively.

The T_1-relaxivities of Gd-DTPA-CMAG-A_2 and Gd-DTPA-CMAG-A_6 in D_2O and 0.725 mM BSA solutions were similar, and the same finding was described by Rebizak et al.[37] This may be attributed to the chemical modification of polysaccharide backbone resulting in greater effect on relaxivity than the length of the spacer arm.

The possibility of Ca^{2+} displacing Gd^{3+} from Gd-DTPA-CMAG-A_n, which may result in the release of the toxic Gd(III) aqua ion in the body,[38] and the relative binding strength to Gd^{3+} of DTPA-CMAG-A_n, EDTA, and DTPA were evaluated by competition studies. Based on the obvious distinction of the T_1-relaxivity between Gd^{3+}, Gd-EDTA, Gd-DTPA, and Gd-DTPA-CMAG-A_2 (Gd-DTPA-CMAG-A_6) in D_2O, 11.8, 8.23, 5.3 and 7.4 (7.3) $mM^{-1}\,s^{-1}$, the existing form of Gd^{3+} in solution after the addition of Ca^{2+}, EDTA, or DTPA may be deduced by the examination of the longitudinal relaxation time T_1. The T_1 of Gd-DTPA-CMAG-A_n in D_2O after adding molar equivalent of Ca^{2+} or EDTA is close to that of the control solution of Gd-DTPA-CMAG-A_n, indicating that Ca^{2+} hardly displaced Gd^{3+} from Gd-DTPA-CMAG-A_n and the relative binding strength to Gd^{3+} of Gd-DTPA-CMAG-A_n is higher than that of EDTA. However, T_1 of Gd-DTPA-CMAG-A_2 (Gd-DTPA-CMAG-A_6) solution after adding molar equivalent of DTPA increased to 1.4 (1.5) times that of the control solution of Gd-DTPA-CMAG-A_2 (Gd-DTPA-CMAG-A_6), suggesting that the relative binding strength to Gd^{3+} of Gd-DTPA-CMAG-A_n is lower than that of DTPA. On the basis of competition studies, the relative binding strength to Gd^{3+} appeared to be DTPA > Gd-DTPA-CMAG-A_n > EDTA. Since the stability constants of Gd-DTPA, Gd-monoamidified DTPA, and Gd-EDTA are $10^{22.46}$, 10^{19}, and $10^{17.35}$,[4,39] respectively, the stability constant of Gd-DTPA-CMAG-A_n should be between 10^{22} and 10^{17}. This is a rational order of stability as expected from the coordinating numbers of carboxyl and nitrogen, which are 5, 4, 4 and 3, 3, 2, for DTPA, Gd-DTPA-CMAG-A_n, and EDTA, respectively.

2.3. In vivo imaging

The MRI signal enhancements of the Wistar rat liver parenchyma and kidney were obtained after the injec-

tion of Gd-DTPA-CMAG-A_2 (0.079 ± 0.002 mmol/kg Gd^{3+}) or Gd-DTPA (0.096 ± 0.003 mmol/kg). Following administration of Gd-DTPA-CMAG-A_2, liver parenchyma showed higher enhancement that persisted throughout the whole imaging periods (Figs. 4 and 5). The signal intensity increased by $38.7 \pm 6.4\%$ within the first 30 min, and a $27.2 \pm 6.7\%$ enhancement was observed in the next 50 min. Compared with a mean percentage enhancement of $21.9 \pm 4.5\%$ for Gd-DTPA during its maximum enhancement time of 20–40 min, that of Gd-DTPA-CMAG-A_2 is higher and prominent.

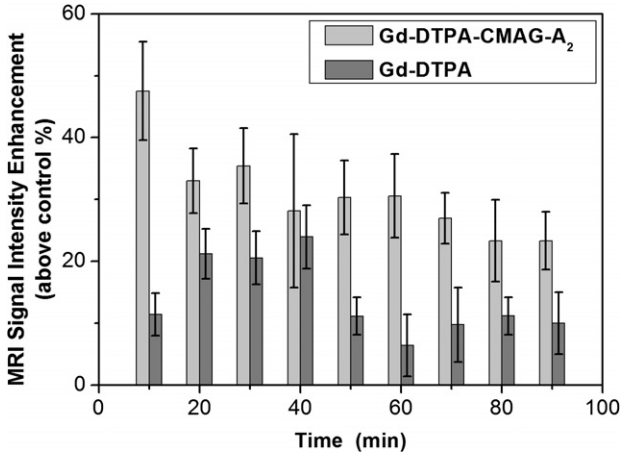

Figure 4. The mean percentage enhancement of liver versus time post-intravenous administration of Gd-DTPA-CMAG-A_2 (light gray bar) and Gd-DTPA (gray bar).

The enhancement patterns in kidney for Gd-DTPA-CMAG-A_2 and Gd-DTPA were very similar. The signal intensity increased shortly after administration, and decreased slowly thereafter (Figs. 6 and 7). The mean percentage enhancement was $69.4 \pm 4.4\%$ and $53.8 \pm 4.8\%$, respectively, for Gd-DTPA-CMAG-A_2 and Gd-DTPA for the first 10–30 min and an enhancement of $53.0 \pm 10.3\%$ and $32.0 \pm 7.1\%$ was observed in the next 60 min, respectively, for Gd-DTPA-CMAG-A_2 and Gd-DTPA.

Although the uptake and excretion of contrast agent are very complex processes, the signal intensity changes ultimately due to distribution (uptake) and elimination (excretion) of the contrast agents, whichever species they are in. We assume that the uptake and the excretion of these agents follow a simplified model shown in Section 4 by using the method of Feng et al.[36]

Data shown in Figures 4 and 6 can be well fitted to the simplified model and the corresponding parameters are listed in Table 2. It shows that the hepatic uptake rate

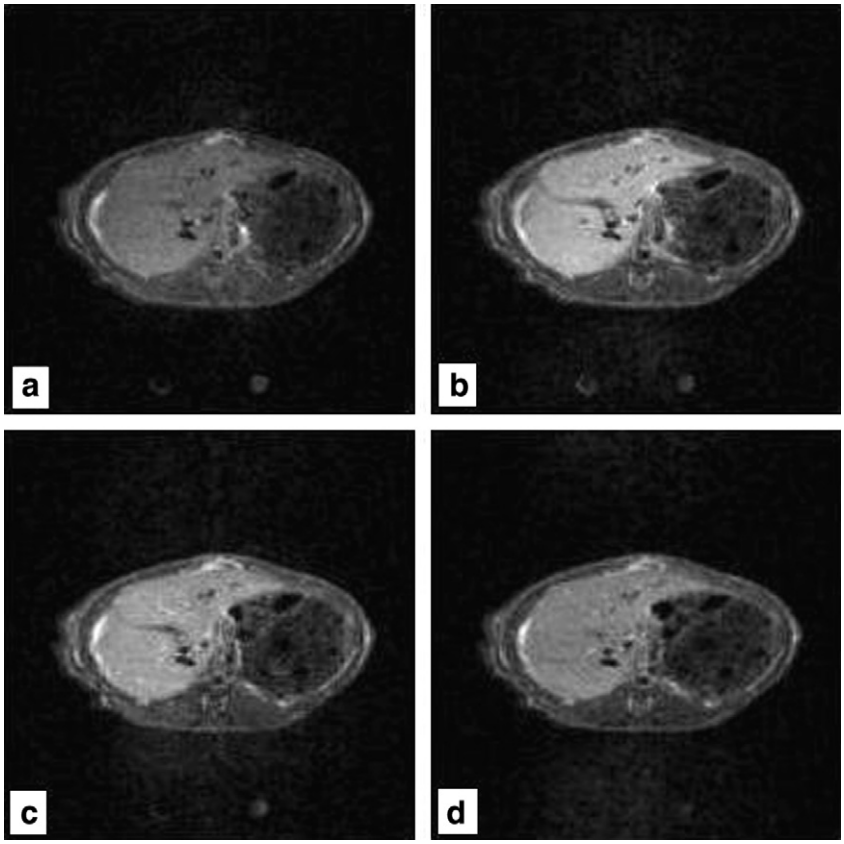

Figure 5. Axial T_{1-w} images of rat liver prior to (a) and, 10 min (b), 35 min (c), 75 min (d) post-intravenous injection of Gd-DTPA-CMAG-A_2 (0.079 ± 0.002 mmol/kg Gd^{3+}) into rat.

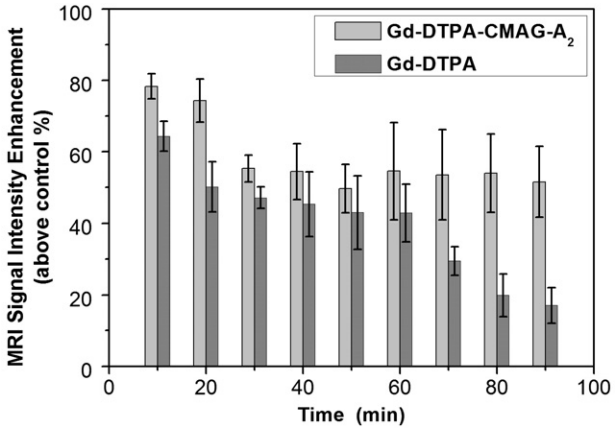

Figure 6. The mean percentage enhancement of kidney versus time post-intravenous administration of Gd-DTPA-CMAG-A_2 (light gray bar) and Gd-DTPA (gray bar).

Table 2. The half-life times of hepatic (renal) uptake and excretion of Gd-DTPA and Gd-DTPA-CMAG-A_2

Gd^{3+} complexes	IE_{max}	$t_{1/2}$, Uptake[a] (min)	$t_{1/2}$, excretion (min)	AF[b]
Liver				
Gd-DTPA	44.3	16.7	52.4	0.3
Gd-DTPA-CMAG-A_2	42.9	0.8	129.8	0.1
Kidney				
Gd-DTPA	69.3	4.6	86.1	0.1
Gd-DTPA-CMAG-A_2	76.6	0.1	153.8	0.1

[a] The $t_{1/2}$ of uptake and excretion were calculated using Solver of Excel 2003 (Microsoft Corp.) according to nonlinear programming.

[b] AF represents the agreement factor between the experimental and calculated hepatic (renal) excretion curves, which is defined as follows: $AF = \sqrt{\frac{\sum(IE_{exp}-IE_{cal})^2}{\sum IE_{exp}^2}}$ where IE_{exp} and IE_{cal} are the experimental and calculated intensity enhancements, respectively.

of Gd-DTPA-CMAG-A_2 ($t_{1/2}$, uptake 0.8 min) is faster than that of Gd-DTPA ($t_{1/2}$, uptake 16.7 min) and the excretion rate of Gd-DTPA-CMAG-A_2 ($t_{1/2}$, excretion 129.8 min) is slower than that of Gd-DTPA ($t_{1/2}$, excretion 52.4 min). Gd-DTPA-CMAG-A_2 shows quicker uptake rate and slower excretion rate than that of Gd-DTPA, implying that Gd-DTPA-CMAG-A_2 may be used as hepatic contrast agents to provide stable imaging contrast for a longer time. Gd-DTPA-CMAG-A_2 produced pronounced effects on liver, probably due to a combination of two effects: (a) A prolonged blood circulation time of the polysaccharide-Gd-DTPA because of their high molecular weight. As the liver is a well-perfused organ, any T_1 effect in blood will give a shortened

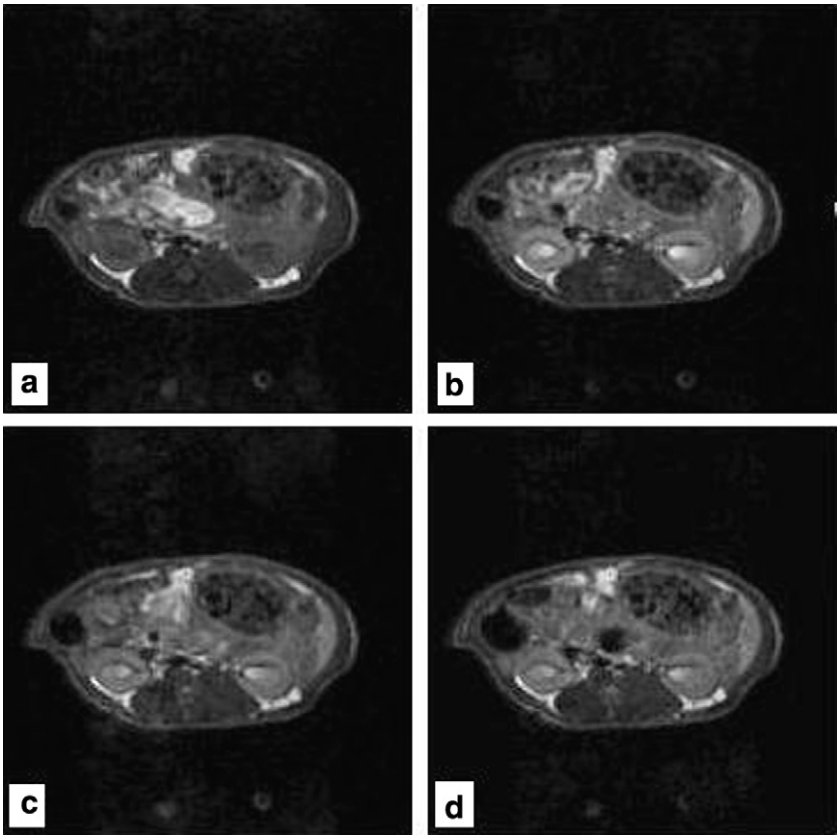

Figure 7. Axial T_{1-w} images of rat kidney prior to (a) and, 10 min (b), 35 min (c), 75 min (d) post-intravenous injection of Gd-DTPA-CMAG-A_2 (0.079 ± 0.002 mmol/kg Gd^{3+}).

T_1 of liver.[40] (b) Arabinogalactan has properties that make it suitable as a carrier for targeting diagnostic or therapeutic agents via the asialoglycoprotein receptor to hepatocytes.[15] In contrast to the rapid rate of metabolism of Gd-DTPA, the animal group receiving Gd-DTPA-CMAG-A_2 displayed an increase in the MR signal intensity in the liver shortly after injection that persisted for a longer time. Therefore, the timing of contrast injection and long data acquisition times become less significant and an optimal imaging window is feasible.

Besides the liver, kidney was significantly enhanced as well, indicating that Gd-DTPA-CMAG-A_2 was also removed from the blood and eliminated through the kidney. Data shown in Figure 6 can be well fitted to the same simplified model. Listed in Table 2 are the corresponding parameters, which showed that the renal uptake rate of Gd-DTPA-CMAG-A_2 ($t_{1/2}$, uptake 0.1 min) is faster than that of Gd-DTPA ($t_{1/2}$, uptake 4.6 min), but the renal excretion rate of Gd-DTPA ($t_{1/2}$, excretion 86.1 min) is faster than that of Gd-DTPA-CMAG-A_2 ($t_{1/2}$, excretion 153.8 min). The low excretion rates of this agent in kidney are accompanied by the fact that renal MRI intensity enhancement of this contrast agent persisted during the whole imaging period. Gd-DTPA-CMAG-A_2 produced higher enhancement than Gd-DTPA in the signal intensity of kidney even at slightly lower injection dosages.

3. Conclusion

In this study, we have synthesized and characterized a new type of macromolecular conjugate consisting of arabinogalactan and Gd-DTPA with higher T_1-relaxivity for use as MRI contrast agents. The polymer contrast agents have good stabilities in vitro in the presence of molar equivalent of Ca^{2+} or EDTA. MR imaging showed that signal intensities from the livers of healthy rats injected with lower doses of Gd-DTPA-CMAG-A_2 were remarkably enhanced for a longer period. Our preliminary in vivo and in vitro study has suggested that Gd-DTPA-CMAG-A_2 could be a potential liver-specific MRI contrast agent.

4. Experimental

4.1. General materials and methods

Arabinogalactan was purchased from Aldrich. 2,4,6-Trinitrobenzene sulfonic acid (TNBS) and 2-ethoxy-1-ethoxycarbonyl-1,2-dihydroquinoline (EEDQ) were acquired from Fluka. Dextran T-10 and T-40 were purchased from Pharmacia. All other reagents (A.R.) were used as received without further purification.

Fourier transform infrared spectra (FTIR) in the range of 4000–400 cm^{-1} were recorded on KBr plate with a Bio-Rad FTS-7 spectrophotometer. The ^{13}C NMR spectrum were recorded in 4:1 water–D_2O at 25 °C, on a Bruker Avance 600 NMR spectrometer. Chemical shifts are expressed in parts per million (ppm) relative to the methyl signal of internal acetone (30.89 ppm).[21] The carboxylate content of carboxymethylarabinogalactan was determined as follows:[26] the sodium salt of CMAG was converted into the acid form by treating it with strongly acidic cation-exchange resin (Type 732, produced in china) and recovered by freeze-drying. A portion of the sample (0.1 g) was dissolved in 20 mL deionized water and a known amount of NaOH was added. The carboxylic acid content was determined by back-titration with 0.1 N HCl using phenolphthalein as an indicator. The amine groups of aminated carboxymethylarabinogalactan were estimated by means of trinitrobenzylsulfonic assay with known concentrations of hexylamine.[41] The DTPA contents were obtained by a reverse complexometric method.[27] Gadolinium content was determined on a TJA POMES inductively coupled plasma mass spectroscopy/spectrophotometer.

4.2. Molecular size of DTPA-CMAG-A_n

The size of DTPA-CMAG-A_n was measured by SEC using a Waters-2414 refractive index detector, Waters Ultrahydrogel 120 and Waters Ultrahydrogel 250 columns (7.8 × 300 mm). The solute was eluted with 0.15 M $NaNO_3$ and 0.01 M NaH_2PO_4 at a flow rate of 0.8 mL/min. Solutions for analysis had a polymer concentration of 3.0 mg/mL and the injection volume was set at 10 μL.

4.3. Stability study

A volume of 0.3 mL of 5 mM Ca^{2+} (pH 5), EDTA (pH 7), or DTPA (pH 7) was added to 0.3 mL of Gd-DTPA-CMAG-A_n solution containing a molar equivalent of Gd^{3+}. Their relaxation times were measured after 24 h and compared with that of 2.5 mM Gd-DTPA-CMAG-A_n D_2O solutions.

4.4. In vitro relaxation time

The solvent longitudinal relaxation times (T_1) for Gd-DTPA-CMAG-A_n in D_2O and BSA (0.725 mM, in D_2O) solution were measured by a standard inversion-recovery pulse sequence on a Bruker Avance 400 NMR spectrometer at 25 °C and 9.4 T. For each complex, five samples were prepared separately with a concentration varying between 0 and 5 mM Gd^{3+} in unbuffered aqueous solution. The ability of proton relaxation enhancement of a paramagnetic compound

is commonly expressed by the term relaxivity r_1, which is defined as the slope of Eq. 1 in the units of $mM^{-1}\,s^{-1}$:

$$(1/T_1)_{obs} = (1/T_1)_d + r_1[M] \quad (1)$$

where $(1/T_1)_{obs}$ and $(1/T_1)_d$ are the observed values in the presence and absence of the paramagnetic species, and [M] is the concentration of the paramagnetic species.

4.5. In vivo imaging

MRI was carried out on three male Wistar rats (200 ± 5 g) for each sample using a Bruker BIOSPEC-47/30 MRI imager at 4.7 T and room temperature. The rats were anesthetized via intraperitoneal injection of 10% urethane solution at 1.0 mL/100 g body weight dose. A series of T_1-weighted images of abdomen were measured after the intravenous injection (thigh vein) of Gd-DTPA-CMAG-A_2 (0.079 ± 0.002 mmol/kg Gd^{3+}) or Gd-DTPA (0.096 ± 0.003 mmol/kg), respectively. In all experiments, imaging was monitored up to 80 min post-contrast injection at intervals of 3 min. Multislice and multiecho (MSME) sequence with repetition time of 300 ms, echo time of 13.6 ms, slice thickness of 2 mm, field of view $5.5 \times 5.5\,cm^2$, and a 128×128 matrix was used for the abdominal scans.

4.6. Imaging analysis

A water tube was placed in the field of view as a phantom reference. The signal intensity (SI) was normalized to that of the phantom (relative signal intensity, RI). The intensity enhancement (IE) at time point t is defined as

$$IE\ (\%) = (RI_{(t)} - RI_{(0)})/RI_{(0)} \times 100 \quad (2)$$

where $RI_{(t)}$ and $RI_{(0)}$ correspond to the normalized signal intensity measured at time point t and pre-contrast, respectively.

We assume that the uptake and the excretion of these agents follow a simplified first-order reaction, that is, the IE in the T_1-weighted images may be expressed in the following equation:

$$IE_t = IE_{max} \times \left[1 - e^{-t/t_{1/2}}\right] \quad (3)$$

where $t_{1/2}$ is the half-life time of uptake or excretion. Since both uptake and excretion take place simultaneously, the observed IE can be expressed as

$$\begin{aligned} IE_{obsd} &= IE_{uptake} - IE_{excretion} \\ &= IE_{max} \times \left[-e^{-t/t_{1/2},uptake} + e^{-t/t_{1/2},excretion}\right] \end{aligned} \quad (4)$$

4.7. Synthesis of Gd-DTPA-arabinogalactans

The modified Rebizak's method[27] was used to synthesize DTPA-CMAG-A_n.

4.7.1. Synthesis of carboxymethylarabinogalactan (CMAG).

AG (6.0 g) was dissolved in 50 mL of 6 N NaOH at 0 °C, then 12.3 g (0.13 mol) of chloroacetic acid was added slowly. The reaction mixture was transferred into a temperature-controlled reactor kept at 60 °C. After 50 min of heating, the mixture was cooled to room temperature. The product was precipitated with methanol and recovered by filtration. The solid was transferred to a dialysis bag (MWCO 6000–8000 g/mol) and dialyzed against deionized water for three days. The residual solution was lyophilized to give CMAG as a slightly yellow crystalline solid. IR (KBr, cm^{-1}): 3413 (O–H), 2924 (C–H), 1604 (C=O carboxylate), 1080 (C–O). ^{13}C NMR (δ/ppm): 178.6–177.7 (–CH_2*C*OONa), 109.9 (C-1/α-Ara*f*), 103.9 (C-1/β-Gal*p*), 83.7–80.1 (C-2–C-4/α-Ara*f*, C-3–C-4/β-Ara*f*), 77.2 (C-2/α-Ara*f*), 75.7 (C-5/β-Gal*p*), 74.1 (C-3/β-Ara*f*), 73.4 (C-3/β-Gal*p*), 71.3 (C-4/β-Gal*p*), 69.3 (C-2/β-Gal*p*), 68.7 (–*C*H_2COONa), 63.9 (C-5/α-Ara*f*), 61.7 (C-6/β-Gal*p*).

4.7.2. Synthesis of aminated carboxymethylarabinogalactan (CMAG-A_2).

CMAG (3.0 g, 6.0 mmol of COO^- groups) was dissolved in 30 mL of deionized water and the pH of the solution was adjusted to 3 with 1 N HCl. Then a 0.3 M solution of EEDQ in methanol (65 mL) was added dropwise. The resulting solution was added to ethylenediamine (4.0 mL, 60 mmol) and kept at room temperature for 6 h. Then it was purified by dialysis for three days. Finally, the residual solution was lyophilized to give CMAG-A_2 as slightly yellow crystalline flakes. IR (KBr, cm^{-1}): 3385 (O–H), 2926 (C–H), 1649 (amide I), 1075 (C–O). ^{13}C NMR (δ/ppm): 178.6–177.7 (–CH_2*C*OONa), 173.7 (–CH_2*C*ONH), 103.8 (C-1/β-Gal*p*), 83.7–80.1 (C-2–C-4/α-Ara*f*, C-3–C-4/β-Ara*f*), 75.7 (C-5/β-Gal*p*), 74.1 (C-3/β-Ara*f*), 73.5 (C-3/β-Gal*p*), 71.6 (C-4/β-Gal*p*), 69.4 (C-2/β-Gal*p*), 63.9 (C-5/α-Ara*f*), 61.6 (C-6/β-Gal*p*), 40.7 (–CH_2CONH*C*$H_2$$CH_2$$NH_2$), 39.9 (–$CH_2$CONHC$H_2$*C*$H_2$$NH_2$).

4.7.3. Synthesis of DTPA-arabinogalactan conjugation (DTPA-CMAG-A_2).

The DTPA succinimidic ester (DTPA-ONSu)[37] was used to couple DTPA covalently to the amino groups of the AG conjugate. After DTPA (8 g, 20.3 mmol) was dissolved in acetonitrile (10 mL) and triethylamine (11.3 mL) mixture, DCC (2.87 g, 14.4 mmol) and HONSu (1.66 g, 14.4 mmol) were added. The reaction mixture was stirred for 90 min at room temperature. After the filtration of dicyclohexyl urea, the filtrate was dropped into a solution of CMAG-A_2 (1 g, 0.51 mmol of NH_2 groups) in 10 mL of deionized water while maintaining a constant pH at 10. The solution was stirred at room temperature for 24 h and the acetonitrile was removed under vacuum. The residual solution was purified by dialysis against deionized water for three days and recovered by

freeze-drying. IR (KBr, cm^{-1}): 3415 (O–H), 2932 (C–H), 1738 (COO^-), 1650 (amide I), 1075 (C–O). ^{13}C NMR (δ/ppm): 179.2 (C-1/DTPA carboxyl), 178.6–177.5 (–CH_2*C*OONa, C-8/DTPA CONH carbon), 173.8 (–CH_2*C*ONH), 171.2 (C-7, C-7′ and C-7″/DTPA carboxyls), 104.0 (C-1/β-Gal*p*), 83.7–80.1 (C-2–C-4/α-Ara*f*, C-3–C-4/β-Ara*f*), 75.7 (C-5/β-Gal*p*), 74.5 (C-3/β-Ara*f*), 73.4 (C-3/β-Gal*p*), 71.2 (C-4/β-Gal*p*), 69.3 (C-2/β-Gal*p*), 63.9 (C-5/α-Ara*f*), 61.7 (C-6/β-Gal*p*), 60.9 (C-5/DTPA CH_2 carbon), 57.7 (C-6, C-6′ and C-6″/DTPA CH_2 carbons), 56.8 (C-2/DTPA CH_2 carbon), 53.6 (C-3 and C-3′/DTPA CH_2 carbons), 49.0 (C-4 and C-4′/DTPA CH_2 carbons), 40.7 (–CH_2CONH*CH_2CH_2*NH).

The arabinogalactan derivative (Gd-DTPA-CMAG-A_6) conjugated by hexylamine was prepared by the above method.

4.7.4. Preparation of gadolinium conjugates (Gd-DTPA-CMAG-A_n). The Gd-DTPA-CMAG-A_n were obtained by mixing $GdCl_3$ with DTPA-CMAG-A_n with a molar ratio Gd^{3+}/DTPA = 1.2. Typically, the mixtures were stirred overnight at room temperature, adjusted with 1 N NaOH solution to pH 5. Xylenol Orange indicator was added into the solution, and EDTA was then added until the pink color disappeared. The polymer conjugates were purified by dextran sephadex G-25 column, and the eluting peak of polysaccharide was detected using a mixture solution of 6% phenol and concentrated sulfuric acid. Finally, the solution was lyophilized to give Gd-DTPA-CMAG-A_n as pale yellow flakes.

Acknowledgments

For financial support, we thank State Key Laboratory of Magnetic Resonance and Atomic and Molecular Physics of China (No. T152004), and Science and Technology Foundation of Changchun City (No. 2005137).

References

1. Rinck, P. A. *Magnetic Resonance Imaging*, 4th ed.; Blackwell Science: Berlin, 2001; p 149.
2. Lauffer, R. B. *Chem. Rev.* **1987**, *87*, 901–927.
3. Aime, S.; Crich, S. G.; Gianolio, E.; Giovenzana, G. B.; Tei, L.; Terreno, E. *Coord. Chem. Rev.* **2006**, *250*, 1562–1579.
4. Caravan, P.; Ellison, J. J.; Mcmurry, T. J.; Lauffer, R. B. *Chem. Rev.* **1999**, *99*, 2293–2352.
5. Barkhausen, J.; Ebert, W.; Debatin, J. F.; Weinmann, H. J. *J. Am. Colloid Cardiol.* **2002**, *39*, 1392–1398.
6. Runge, V. M. *J. Magn. Reson. Imaging* **2000**, *12*, 205–213.
7. Bottrill, M.; Nicholas, L. K.; Long, N. J. *Chem. Soc. Rev.* **2006**, *35*, 557–571.
8. Uggeri, F.; Aime, S.; Anelli, P. L.; Botta, M.; Brocchetta, M.; Dehaen, C.; Ermondi, G.; Grandi, M.; Paoli, P. *Inorg. Chem.* **1995**, *34*, 633–643.
9. Schmitt-Willich, H.; Brehm, M.; Ewers, C. L. J.; Michl, G.; Muller-Fahrnow, A.; Petrov, O.; Platzek, J.; Raduchel, B.; Sulzle, D. *Inorg. Chem.* **1999**, *38*, 1134–1144.
10. Anelli, P. L.; Lattuada, L.; Lorusso, V.; Lux, G.; Morisetti, A.; Morosini, P.; Serleti, M.; Uggeri, F. *J. Med. Chem.* **2004**, *47*, 3629–3641.
11. Thompson, M. K.; Misselwitz, B.; Tso, L. S.; Doble, D. M. J.; Schmitt-Willich, H.; Raymond, K. N. *J. Med. Chem.* **2005**, *48*, 3874–3877.
12. Gallez, B.; Lacour, V.; Demeure, R.; Debuyst, R.; Dejehet, F.; Dekeyser, J. L.; Dumont, P. *Magn. Reson. Imaging* **1994**, *12*, 61–69.
13. Reimer, P.; Weissleder, R.; Brady, T. J.; Yeager, A. E.; Baldwin, B. H.; Tennant, B. C.; Wittenberg, J. *Radiology* **1991**, *180*, 641–645.
14. Prata, M. I. M.; Santos, A. C.; Torres, S.; Andre, J. P.; Martins, J. A.; Neves, M.; Garcia-Martin, M. L.; Rodrigues, T. B.; Lopez-Larrubia, P.; Cerdan, S.; Geraldes, C. F. G. C. *Contrast Med. Mol. Imaging* **2006**, *1*, 246–258.
15. Groman, E. V.; Enriquez, P. M.; Jung, C.; Josephson, L. *Bioconjugate Chem.* **1994**, *5*, 547–556.
16. Falk, R.; Domb, A. J.; Polacheck, I. *Antimicrob. Agents Chemother.* **1999**, *43*, 1975–1981.
17. Tanaka, T.; Fujishima, Y.; Hamano, S.; Kaneo, Y. *Eur. J. Pharm. Sci.* **2004**, *22*, 435–444.
18. Sun, G. Y.; Feng, J. H.; Jing, F. Y.; Pei, F. K.; Liu, M. L. *J. Magn. Magn. Mater.* **2003**, *265*, 123–129.
19. Sun, G. Y.; Feng, J. H.; Jing, F. Y.; Pei, F. K. *Chem. J. Chin. U.* **2002**, *23*, 1837–1841.
20. Clarke, A. E.; Anderson, R. L.; Stone, B. A. *Phytochemistry* **1979**, *18*, 521–540.
21. Suarez, E. R.; Kralovec, J. A.; Noseda, M. D.; Ewart, H. S.; Barrow, C. J.; Lumsden, M. D.; Grindley, T. B. *Carbohydr. Res.* **2005**, *340*, 1489–1498.
22. Karacsonyi, S.; Kovacik, V.; Alfoldi, J.; Kubackova, M. *Carbohydr. Res.* **1984**, *134*, 265–274.
23. Odonmazig, P.; Ebringerova, A.; Machova, E.; Alfoldi, J. *Carbohydr. Res.* **1994**, *252*, 317–324.
24. Huynh, R.; Chaubet, F.; Jozefonvicz, J. *Carbohydr. Res.* **2001**, *332*, 75–83.
25. Yan, G. P.; Hu, B.; Liu, M. L.; Li, L. Y. *J. Pharm. Pharmacol.* **2005**, *57*, 351–357.
26. Verraest, D. L.; Peters, J. A.; Batelaan, J. G.; Vanbekkum, H. *Carbohydr. Res.* **1995**, *271*, 101–112.
27. Rebizak, R.; Schaefer, M.; Dellacherie, E. *Bioconjugate Chem.* **1997**, *8*, 605–610.
28. Bligh, S. W. A.; Harding, C. T.; Sadler, P. J.; Bulman, R. A.; Bydder, G. M.; Pennock, J. M.; Kelly, J. D.; Clatham, I. A.; Marriott, J. A. *Magn. Reson. Med.* **1991**, *17*, 516–532.
29. Feng, J. H.; Sun, G. Y.; Pei, F. K.; Liu, M. L. *Bioorg. Med. Chem.* **2003**, *11*, 3359–3366.
30. Lebduskova, P.; Kotek, J.; Hermann, P.; Elst, L. V.; Muller, R. N.; Lukes, I.; Peters, J. A. *Bioconjugate Chem.* **2004**, *15*, 881–889.
31. Armitage, F. E.; Richardson, D. E.; Li, K. C. P. *Bioconjugate Chem.* **1990**, *1*, 365–374.
32. Wiener, E. C.; Brechbiel, M. W.; Brothers, H.; Magin, R. L.; Gansow, O. A.; Tomalia, D. A.; Lauterbur, P. C. *Magn. Reson. Med.* **1994**, *31*, 1–8.
33. Langereis, S.; Dirksen, A.; Hackeng, T. M.; van Genderen, M. H. P.; Meijer, E. W. *New J. Chem.* **2007**, *31*, 1152–1160.
34. Li, X. Y.; Li, X. J.; Zhang, S. R.; Pei, F. K. *Polyhedron* **1999**, *18*, 695–697.
35. Reuben, J. *Biochemistry* **1971**, *10*, 2834–2838.

36. Feng, J. H.; Sun, G. Y.; Pei, F. K.; Liu, M. L. *J. Inorg. Biochem.* **2002**, *92*, 193–199.
37. Rebizak, R.; Schaefer, M.; Dellacherie, E. *Bioconjugate Chem.* **1998**, *9*, 94–99.
38. Tweedle, M. F.; Hagan, J. J.; Kumar, K.; Mantha, S.; Chang, C. A. *Magn. Reson. Imaging* **1991**, *9*, 409–415.
39. Sherry, A. D.; Cacheris, W. P.; Kuan, K.-T. *Magn. Reson. Med.* **1988**, *8*, 180–190.
40. Fossheim, S. L.; Kellar, K. E.; Mansson, S.; Colet, J. M.; Rongved, P.; Fahlvik, A. K.; Klaveness, J. *J. Magn. Reson. Imaging* **1999**, *9*, 295–303.
41. Habeeb, A. F. S. A. *Anal. Biochem.* **1966**, *14*, 328–336.